


ECM stiffness regulates calcium influx into mitochondria via tubulin and VDAC1 activity

Minji Kim^a, Kiseok Han^a, Gyuho Choi^a, Sanghyun Ahn^a, Jung-Soo Suh^a and Tae-Jin Kim ^{a,b,c,d}

^aDepartment of Integrated Biological Science, College of Natural Sciences, Pusan National University, Busan, Republic of Korea; ^bDepartment of Biological Sciences, College of Natural Sciences, Pusan National University, Busan, Republic of Korea; ^cNuclear Science Research Institute, Pusan National University, Busan, Republic of Korea; ^dInstitute of Systems Biology, Pusan National University, Busan, Republic of Korea

ABSTRACT

Calcium ions (Ca^{2+}) play pivotal roles in regulating numerous cellular functions, including metabolism and growth, in normal and cancerous cells. Consequently, Ca^{2+} signaling is a vital determinant of cell fate and influences both cell survival and death. These intracellular signals are susceptible to modulation by various factors, including changes in the extracellular environment, which leads to mechanical alterations. However, the effect of extracellular matrix (ECM) stiffness variations on intracellular Ca^{2+} signaling remains underexplored. In this study, we aimed to elucidate the mechanisms of Ca^{2+} regulation through the mitochondria, which are crucial to Ca^{2+} homeostasis. We investigated how Ca^{2+} regulatory mechanisms adapt to different levels of ECM stiffness by simultaneously imaging the mitochondria and endoplasmic reticulum (ER) in live cells using genetically encoded biosensors. Our findings revealed that the uptake of mitochondrial Ca^{2+} through Voltage-Dependent Anion Channel 1 (VDAC1), facilitated by intracellular tubulin, is influenced by ECM stiffness. Unraveling these Ca^{2+} regulatory mechanisms under various conditions offers a novel perspective for advancing biomedical studies involving Ca^{2+} signaling.

ARTICLE HISTORY

Received 11 April 2024
Revised 15 July 2024
Accepted 9 August 2024

KEYWORDS

ECM stiffness; calcium; mitochondria; live cell imaging; VDAC1


Introduction

Ca^{2+} is an integral second messenger within cells, orchestrating a plethora of cellular mechanisms and pathways, such as muscle contraction, nerve transmission, hormone secretion, communication between organelles, cellular metabolism, and cell growth (Oh 2023; Kim et al., 2023). Among the various cellular organelles, mitochondria are pivotal for the regulation of intracellular Ca^{2+} through their capacity to sequester and release Ca^{2+} . Within the mitochondria, Ca^{2+} functions as a crucial effector molecule, influencing a broad spectrum of Ca^{2+} -dependent processes, including energy production and apoptosis (Giorgi et al. 2018). The primary route of Ca^{2+} uptake into the mitochondria is via transfer from the ER, facilitated by the mitochondria-associated membrane (MAM), which is positioned close to the mitochondria within the ER (Kerkhofs et al. 2018; Missiroli et al. 2018; Kim et al., 2023; Kwon et al. 2023). The release of Ca^{2+} from the ER is initiated by the binding of inositol 1,4,5-trisphosphate (IP3) to its receptors on the ER membrane, with the liberated Ca^{2+}

subsequently absorbed by mitochondria through channels in the outer mitochondrial membrane (OMM) (Patergnani et al. 2011). The membrane potential ($\Delta\Psi$), generated by the mitochondrial respiratory chain, provides the electrochemical force required for Ca^{2+} to enter the mitochondrial matrix (Giorgi et al. 2018).

Ca^{2+} signaling is also pivotal in the tumor microenvironment (TME) for the regulation of various physiological processes involved in tumor growth, invasion, and metastasis, affecting both normal and cancerous cells. The TME can influence tumor cell behavior through changes in Ca^{2+} signaling, thereby promoting tumor progression (Monteith et al. 2017). Given its significant effects on cancer cells, strategies that manipulate Ca^{2+} levels to induce apoptosis are currently under investigation (Giorgi et al. 2015). In addition, the TME is dynamic, with factors, such as extracellular matrix (ECM) stiffness, representing the mechanical microenvironment, varying across tissue types, and influencing tumor progression by inducing functional cellular changes (Deng et al. 2022; Park et al. 2023). However,

CONTACT Tae-Jin Kim  tjkim77@pusan.ac.kr  Department of Biological Sciences, College of Natural Sciences, Pusan National University, Busan 46241, Republic of Korea

 Supplemental data for this article can be accessed online at <https://doi.org/10.1080/19768354.2024.2393811>.

© 2024 The Author(s). Published by Informa UK Limited, trading as Taylor & Francis Group

This is an Open Access article distributed under the terms of the Creative Commons Attribution-NonCommercial License (<http://creativecommons.org/licenses/by-nc/4.0/>), which permits unrestricted non-commercial use, distribution, and reproduction in any medium, provided the original work is properly cited. The terms on which this article has been published allow the posting of the Accepted Manuscript in a repository by the author(s) or with their consent.

the underlying mechanisms by which Ca^{2+} signaling responds to different ECM stiffness levels remain largely unexplored. Consequently, a deeper understanding of the regulatory mechanisms governing intracellular Ca^{2+} and mitochondrial control under various conditions represents a crucial avenue for biomedical research, potentially offering new strategies for targeting intracellular Ca^{2+} mechanistically.

In this study, we established environments with varying ECM stiffness and utilized an intensitometer biosensor to monitor changes in Ca^{2+} within the ER and mitochondria to elucidate how mitochondrial Ca^{2+} mechanisms adapt to changes in ECM stiffness. Our findings reveal distinct patterns of mitochondrial Ca^{2+} uptake across varying degrees of matrix stiffness, revealing the regulatory role of intracellular tubulins in this process.

Materials and methods

Cell culture and transfection

HeLa cells were cultured in Dulbecco's Modified Eagle Medium (DMEM; CM002-050, GenDEPOT, Katy, TX, USA) enriched with 10% fetal bovine serum (FBS; 16000-044, Gibco, Waltham, MA, USA), 100 U/ml penicillin, and 100 $\mu\text{g}/\text{mL}$ streptomycin (CA005, GenDepot), in a humidified incubator at 37°C with 5% CO_2 . For transfection, HeLa cells were introduced into DNA plasmids [pCMV CEPIA2 mt (Addgene #58218) and pCMV R-CEPIA1er (Addgene #58216)] using the PEIpro transfection reagent (115-0015, Polyplus, France), following the manufacturer's instructions, and incubated overnight.

Preparation of the polyacrylamide gel

To prepare the polyacrylamide gel, the surface of a confocal dish (model 100350; SPL Life Sciences, Republic of Korea) was treated with 3-aminopropyltrimethoxysilane (catalog number 22589; Thermo Fisher Scientific) for 6 min. The dish was then rinsed with distilled water and treated with 0.5% glutaraldehyde solution (catalog number 27372-1230, Tokyo, Japan) for 30 min. This treatment was followed by a rinse with distilled water. The dish was treated with 3-aminopropyltrimethoxysilane and glutaraldehyde to enhance adhesion between the dish surface and the polyacrylamide gel. To create the polyacrylamide gel, a 40% acrylamide solution (catalog number 161-0140, Bio-Rad, San Francisco, CA, USA) was used, with specific volumes added based on the desired mechanical strength of the gel: 62.5 μl for a gel with 1 kPa stiffness, and 100 μl for a gel with 40 kPa stiffness. Additionally, a 2% bis solution (catalog number 161-0142, Bio-Rad) was added, with 7.5 μl for

1 kPa and 120 μl for 40 kPa. The concentrations of acrylamide and bis determined the mechanical strengths of the gels. The polymerization process involved the addition of 10% ammonium persulfate (APS) solution (catalog number TLP-109.1, Translab, Republic of Korea) and N,N,N',N'-Tetramethylethylenediamine (TEMED; catalog number T1004, Biosesang, Republic of Korea) in the presence of 10 mM HEPES buffer (catalog number GB10-12, Dojindo, Kumamoto, Japan) as described by Kim et al. (2009). The resulting gel solution was then applied to the prepared confocal dish and spread evenly using a 12 mm \varnothing cover glass. After the gel solidified, the dish was filled with distilled water to facilitate the removal of the cover glass.

ECM simulation on polyacrylamide gels

Sulfo-SANPAH (sulfosuccinimidyl 6(4'-azide-2'-nitrophenylamino) hexanoate; catalog number 22589; Thermo Fisher Scientific) was applied to the surface of the gel and exposed to UV light for 6 min. After UV exposure, gels were washed with 100 mM HEPES buffer. This treatment enhanced the adhesion of ECM proteins, which were later added to the gel. Next, a solution of Collagen I (0.2 mg/ml) (Corning[®] Collagen I, Rat Tail; catalog number 354236, BD) was layered onto the treated gel. The gel was then incubated overnight at 4°C to create a simulated ECM environment.

Cell transfer and seeding

Transfected cells were transferred to polyacrylamide gel-coated confocal dishes 5 h before live cell imaging. This duration was chosen to allow sufficient time for the cells to adequately adhere to the gel surface. In scenarios requiring pre-treatment, the cells were first seeded onto the gel-coated surfaces of confocal dishes. We then allowed a settling period for cell attachment, followed by the administration of pre-treatment for a predetermined duration. During the seeding process, precision was paramount, and a 10 μl pipette was utilized to facilitate the deposition of single cells for imaging.

Pre-imaging preparation

Prior to initiating the imaging process, the cells positioned within the confocal dishes were washed with phosphate-buffered saline (PBS; LB004-02; WELGENE, Republic of Korea) to remove any residual media or debris. Subsequently, to ensure optimal cell viability and conditions during the imaging phase, standard DMEM was replaced with a CO_2 -independent medium (18045-088, Gibco). This specialized medium was

fortified with 0.5% FBS, 4 mM L-glutamine, 100 U/mL penicillin, and 100 µg/mL streptomycin, catering to the nutritional and environmental needs of the cells in the absence of CO₂.

Microscopy and image acquisition

Imaging was performed using a Leica DMI8 microscope equipped with a charge-coupled device (CCD) camera (DFC450C; Leica). For the visualization of EGFP expressed from pCMV CEPIA2 mt, the setup included a 475/30 nm excitation filter, a 500 nm dichroic mirror, and a 535/30 nm emission filter. For mCherry expressed from pCMV R-CEPIA1er, a 575/20 nm excitation filter, 598 nm dichroic mirror, and 642/80 nm emission filter were utilized. The filter changes were automated using a filter changer mechanism. To normalize the emission intensity data, the GFP and RFP values were each divided by their respective average values obtained 5 min prior to ionomycin treatment. This approach allowed for the correction of fluorescence intensity fluctuations and facilitated a standardized comparison across different experimental conditions.

Statistical analysis

Statistical analyses were performed using GraphPad Prism, version 10 (GraphPad Software, San Diego, CA, USA). Data are expressed as mean ± standard error of the mean (SEM). To compare two independent groups, unpaired t-tests and Mann–Whitney U tests were used as appropriate, followed by tests for normality and log-normality. The choice of test depended on the distribution of the data. Statistical significance was defined as * $P < 0.05$, ** $P < 0.01$. Values with $P > 0.05$ were considered not statistically significant (ns).

Results

Verification of substrate stiffness differences in polyacrylamide gels

Before proceeding with the full-scale experiments, we verified that the created polyacrylamide gels exhibited the intended differences in substrate stiffness. To determine the stiffness differences between the 1 and 40 kPa substrates, we initially employed Cyto-FAK (Addgene #78300) to observe focal adhesion kinase (FAK) activity across the two stiffness conditions (Supplementary Figure S1), as described by Seong et al. (2011). The results indicated that FAK activity was significantly higher on a stiffer substrate (40 kPa) than on a softer substrate (1 kPa). Furthermore, we used pEGFP-C3-

hYAP1 (Addgene #17843) to validate the differences in substrate stiffness (Supplementary Figure S1) following the methodology described by Franklin et al. (2020). By comparing the nucleus-to-cytoplasm ratio of YAP1, we found that this ratio was significantly elevated on the 40 kPa substrate relative to the 1 kPa substrate. These results confirm that the polyacrylamide gels exhibit the intended range of substrate stiffness, thereby ensuring that subsequent experiments can be conducted in environments with distinct mechanical properties.

Influence of ECM stiffness on mitochondrial Ca²⁺ influx

The primary route of Ca²⁺ influx into mitochondria is mediated by the release of Ca²⁺ from the endoplasmic reticulum (ER). To simultaneously investigate the dynamic changes in Ca²⁺ in the ER and mitochondria, we employed ER-targeted (pCMV R-CEPIA1er) and mitochondrial-targeted (pCMV CEPIA2 mt) Ca²⁺ sensors along with ionomycin to induce Ca²⁺ concentration changes in each organelle (Suzuki et al. 2014; Seegren et al. 2023). These biosensors function by binding calmodulin to Ca²⁺ within organelles, causing a conformational change in the EF-hand motif and resulting in an increase in the fluorescence intensity of the fluorescent protein. This change was visualized as an increase in the brightness and intensity of the sensor via live cell imaging (Figure 1A, C). In experiments conducted under soft gel conditions (1 kPa), ionomycin treatment decreased ER Ca²⁺ levels without a corresponding increase in mitochondrial Ca²⁺ levels (Figure 1B). Conversely, under stiff gel conditions (40 kPa), the ionomycin-induced depletion of ER Ca²⁺ was accompanied by significant spikes in mitochondrial Ca²⁺ influx (Figure 1D). This observed pattern of Ca²⁺ dynamics aligns with the rapid release of Ca²⁺ from the ER, followed by its transfer to the mitochondria, which is consistent with findings from previous studies (Ichas et al. 1997; Zamaraeva et al. 2007; Ashrafi et al. 2020; Hotka et al. 2020). These results confirm that substrate stiffness significantly influences the efficiency of Ca²⁺ transfer between the ER and mitochondria.

Role of microtubules in modulating mitochondrial Ca²⁺ channel activity

Building on our initial observations (Figure 1), we hypothesized that ECM stiffness affects mitochondrial Ca²⁺ channel functionality. This hypothesis was inspired by existing research indicating that tubulin regulates channels that facilitate Ca²⁺ entry into the mitochondria (Maldonado et al. 2010). To test this hypothesis, we investigated whether a reduction in intracellular

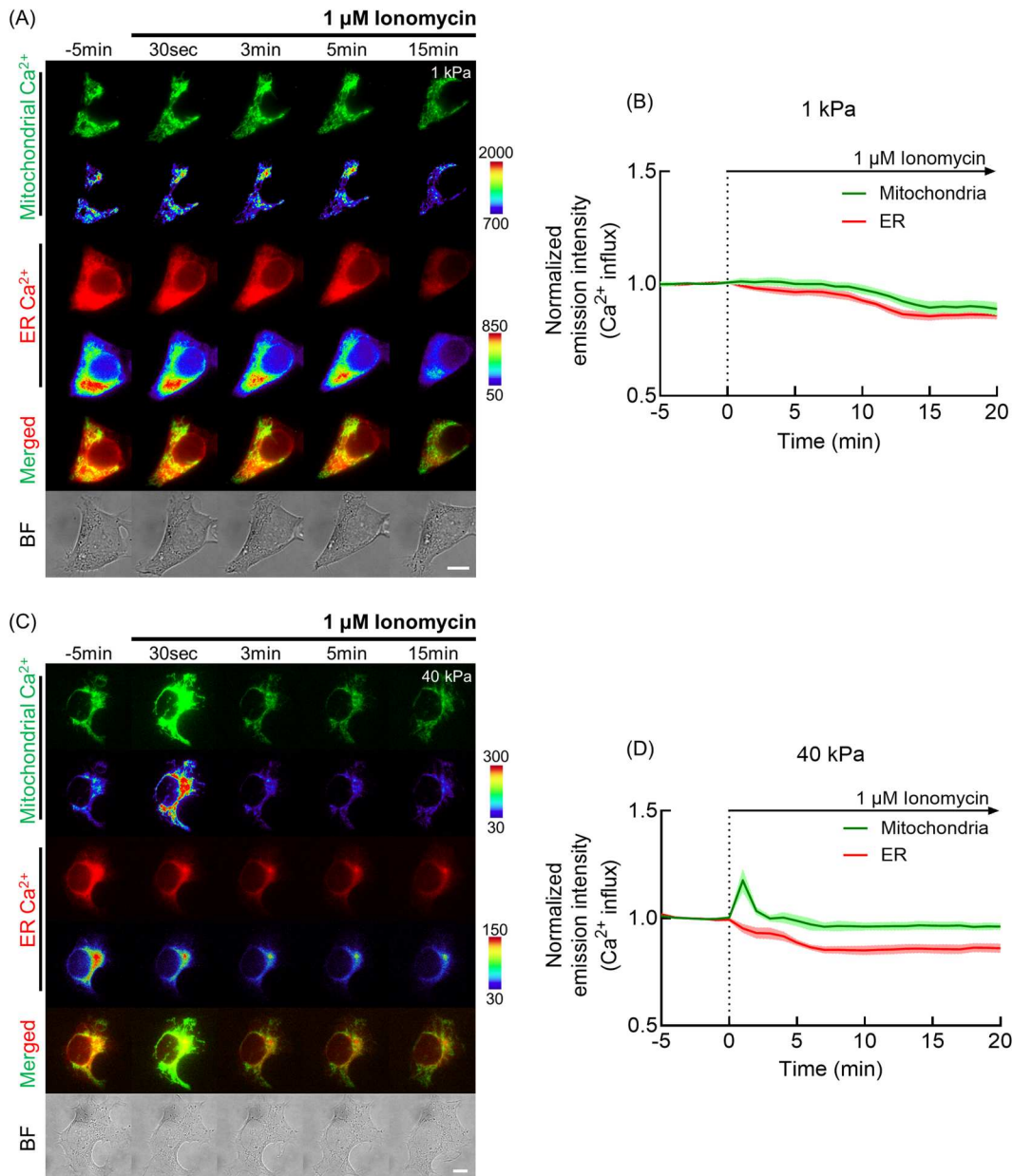


Figure 1. Impact of ECM stiffness on mitochondrial calcium influx. (A, C) Live imaging time-lapse series capturing the intensity of calcium-specific biosensors within HeLa cells: pCMV CEPIA2 mt for mitochondrial calcium (green) and pCMV R-CEPIA1er for endoplasmic reticulum (ER) calcium (red), post-treatment with 1 μM ionomycin on substrates with 1 and 40 kPa stiffness. Ionomycin was administered 5 min after initiating the imaging process, with only the media and cells present in the confocal dish during the initial 5 min. The accompanying color scale bar represents calcium levels, with red indicating high and blue denoting low calcium concentrations (scale bar = 10 μm). (B, D) Quantitative analysis of the time courses of normalized emission intensity from the pCMV CEPIA2 mt and pCMV R-CEPIA1er biosensors in HeLa cells treated with 1 μM ionomycin on substrates with 1 and 40 kPa stiffness. Each line represents the mean value of normalized emission intensity for a group of 10 cells ($n = 10$), and the error bars reflect the standard error of the mean (SEM), illustrating the dynamic calcium changes in response to ECM stiffness and ionomycin treatment.

tubulin levels enhanced mitochondrial Ca^{2+} uptake under conditions of low ECM stiffness (1 kPa). Paclitaxel, a microtubule stabilizer, was used to reduce the intracellular tubulin levels. Subsequently, live-cell imaging was employed to observe changes in mitochondrial Ca^{2+} influx upon ionomycin treatment under different ECM stiffness conditions (Figure 2A, C) (Ojeda-Lopez

et al. 2014). Under soft gel conditions (1 kPa), pretreatment with paclitaxel prior to ionomycin exposure significantly increased mitochondrial Ca^{2+} influx, which correlated with Ca^{2+} release from the ER (Figure 2B). For stiff gels (40 kPa), paclitaxel pretreatment combined with ionomycin administration also enhanced mitochondrial Ca^{2+} levels compared with the baseline, as

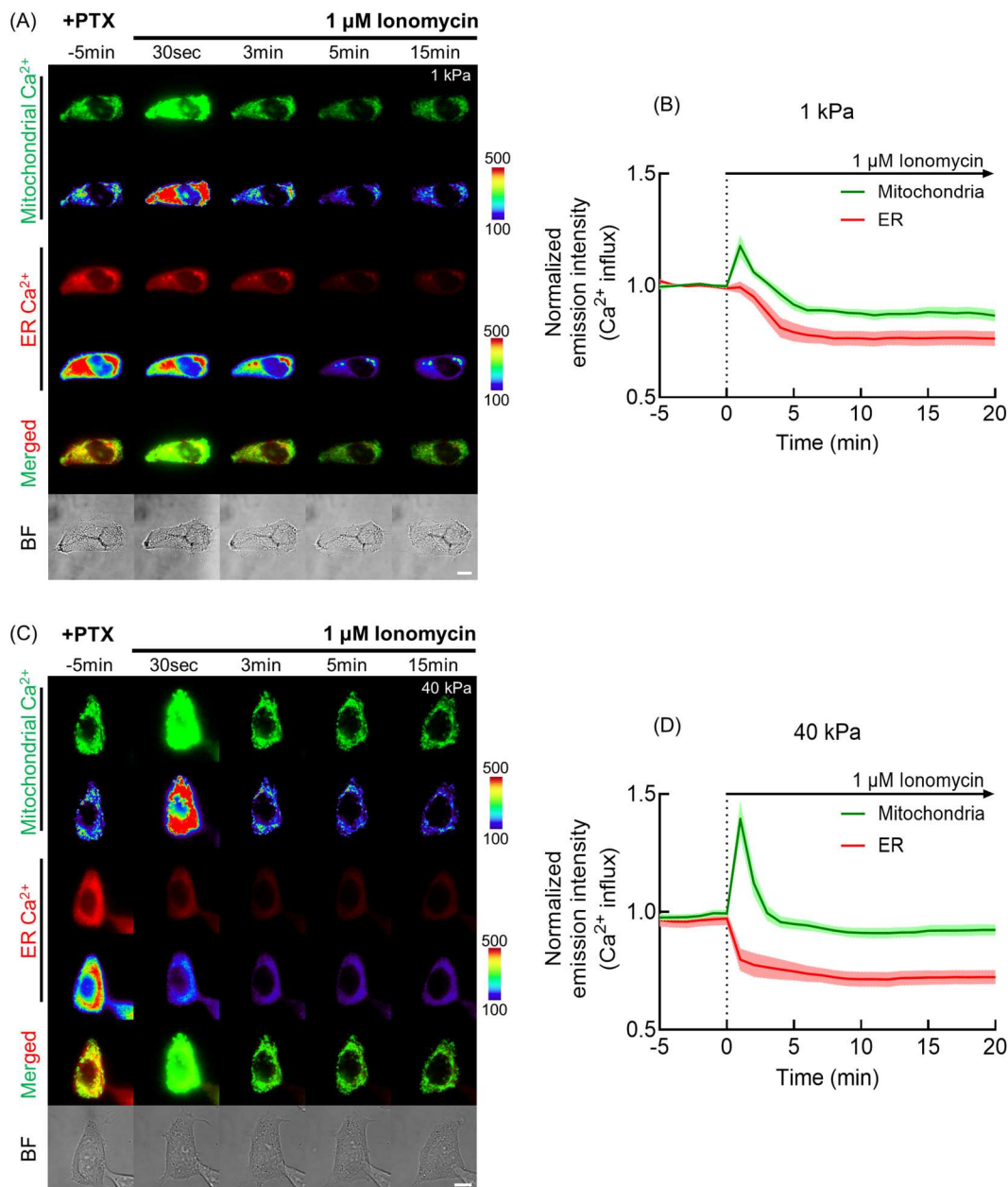


Figure 2. Role of microtubules in enhancing mitochondrial calcium channel function. (A, C) Time-lapse imaging of the fluorescence calcium indicators within HeLa cells: pCMV CEPIA2 mt for mitochondria (green) and pCMV R-CEPIA1er for the ER (red), under 1 and 40 kPa substrate stiffness, respectively. Cells were pre-treated with 10 μM paclitaxel for 20 min, followed by a PBS wash and subsequent exposure to 1 μM Ionomycin. Ionomycin administration occurred after the initiation of live imaging, with only the media and cells present within the confocal dish for the initial 5 min. The color scale indicates calcium concentration levels, with red for high and blue for low (scale bar = 10 μm). (B) Analysis of the temporal changes in normalized emission intensity from pCMV CEPIA2 mt and pCMV R-CEPIA1er in HeLa cells on a 1 kPa substrate treated with 1 μM Ionomycin, showing mean values for a group of 10 cells ($n = 10$). (D) Temporal changes in normalized emission intensity from pCMV CEPIA2 mt and pCMV R-CEPIA1er in HeLa cells on a 40 kPa substrate treated with 1 μM Ionomycin, for a group of nine cells ($n = 9$). In both (B) and (D), lines represent the mean normalized emission intensity, with error bars depicting the standard error of the mean (SEM), which shows the microtubule-mediated modulation of calcium channel activity in response to mechanical stiffness and Ionomycin treatment.

shown in Figure 1 (Figure 2D). These findings suggest that ECM stiffness influences mitochondrial Ca^{2+} uptake, and that reducing intracellular tubulin levels can enhance this process, particularly under conditions of low ECM stiffness.

The impact of tubulin on mitochondrial Ca^{2+} channels

In our ongoing investigation into the mechanisms regulating mitochondrial Ca^{2+} uptake, we explored the role

of increased intracellular tubulin levels in mitochondrial Ca^{2+} channels. This aspect of our study was inspired by previous findings showing that tubulin plays a significant role in modulating these channels (Spencer et al. 1999). To increase intracellular tubulin levels, we used nocodazole, a microtubule-depolymerizing agent known to elevate free tubulin concentrations within cells. We used live-cell imaging to observe the effects of nocodazole treatment, followed by ionomycin exposure, on ER and mitochondrial Ca^{2+} dynamics. The intensity changes in the sensors for both organelles were recorded (Figure 3A, C). In a soft gel environment (1 kPa), nocodazole treatment followed by ionomycin exposure resulted in a significant release of Ca^{2+} from the ER. However, this increase in mitochondrial Ca^{2+} influx was notably reduced (Figure 3B). This suggests that, despite the availability of released Ca^{2+} from the ER, elevated intracellular tubulin levels impede efficient Ca^{2+} transfer to the mitochondria. Similarly, in a stiff gel environment (40 kPa), nocodazole treatment led to a detectable decrease in Ca^{2+} levels in the ER. However, the ionomycin-induced Ca^{2+} influx into the mitochondria was minimal (Figure 3D). These findings indicate that even under conditions that promote ER Ca^{2+} release, increased intracellular tubulin levels hinder the effective uptake of Ca^{2+} by the mitochondria. Our results demonstrate that increased intracellular tubulin levels induced by nocodazole treatment significantly affect mitochondrial Ca^{2+} channel activity. In both soft and stiff gel environments, elevated tubulin levels impair Ca^{2+} influx into mitochondria following ER Ca^{2+} release. This suggests a critical regulatory role for tubulin in mitochondrial Ca^{2+} uptake, highlighting the complex interplay between cytoskeletal elements and mitochondrial function.

Regulation of VDAC1 by ECM stiffness and its role in mitochondrial Ca^{2+} influx

In this study, we aimed to determine whether VDAC1 serves as a primary channel for mitochondrial Ca^{2+} influx, and whether its activity is modulated by tubulin and potentially influenced by ECM stiffness (De Stefani et al. 2012; Ben-Hail et al. 2016). To test this hypothesis, we used NSC15364, a compound known to inhibit VDAC1 by preventing oligomerization (Wu et al. 2023; Zhang et al. 2023). Pretreatment with NSC15364 allowed us to observe changes in Ca^{2+} influx into the mitochondria via live-cell imaging following ionomycin treatment (Figure 4A, C). Our results demonstrated that ionomycin treatment induces Ca^{2+} release from the ER in environments with both low (1 kPa) and high (40 kPa) ECM stiffness. However,

despite this release, there was a minimal increase in mitochondrial Ca^{2+} levels post-treatment when cells were pretreated with NSC15364 (Figure 4B, D). This observation suggests that VDAC1 plays a critical role in mitochondrial Ca^{2+} uptake, and that its inhibition by NSC15364 effectively blocks this influx. To further understand the effects of the different experimental conditions on Ca^{2+} dynamics within the ER and mitochondria, we conducted a comprehensive analysis. ER Ca^{2+} release was evaluated by calculating the changes in the normalized release intensity after ionomycin treatment compared with baseline levels. The analysis revealed no significant differences in ER Ca^{2+} release across all the experimental conditions (Figure 5A). Similarly, we assessed the mitochondrial Ca^{2+} uptake. Under standard conditions, without any pretreatment, a significant increase in mitochondrial Ca^{2+} uptake was observed only at high ECM stiffness (40 kPa). However, when cells were pretreated with paclitaxel, a microtubule stabilizer, there was a notable enhancement in mitochondrial Ca^{2+} uptake, even at low ECM stiffness (1 kPa), showing a significant increase compared to conditions without any pretreatment (Figure 5B). This suggests that microtubules facilitate mitochondrial Ca^{2+} uptake, and that their stabilization by paclitaxel can modulate this process under varying ECM stiffness conditions.

In summary, our study highlights the crucial role of VDAC1 in mitochondrial Ca^{2+} influx and illustrates how its activity is modulated by tubulin and ECM stiffness. The use of NSC15364 confirmed the essential function of VDAC1 in Ca^{2+} uptake, and the influence of tubulin on the regulation of this process was evident, particularly under different ECM stiffness conditions (Figure 5C, D). These findings provide deeper insight into the complex regulation of mitochondrial Ca^{2+} dynamics and the interplay between cytoskeletal elements and mitochondrial function.

Discussion

Calcium signaling plays a critical role in regulating a wide array of cellular processes, including metabolism, growth, and physiological responses, in both normal and cancer cells. This signaling pathway is involved in tumor progression and influences growth, invasion, and metastasis (Monteith et al. 2017). Although disruptions in Ca^{2+} signaling are linked to various diseases, including cancer, the specific intracellular mechanisms driven by environmental and genetic changes remain to be fully elucidated (Giorgi et al. 2018). In our study, we employed polyacrylamide gels to control ECM stiffness, and intensitometric biosensors, pCMV R-

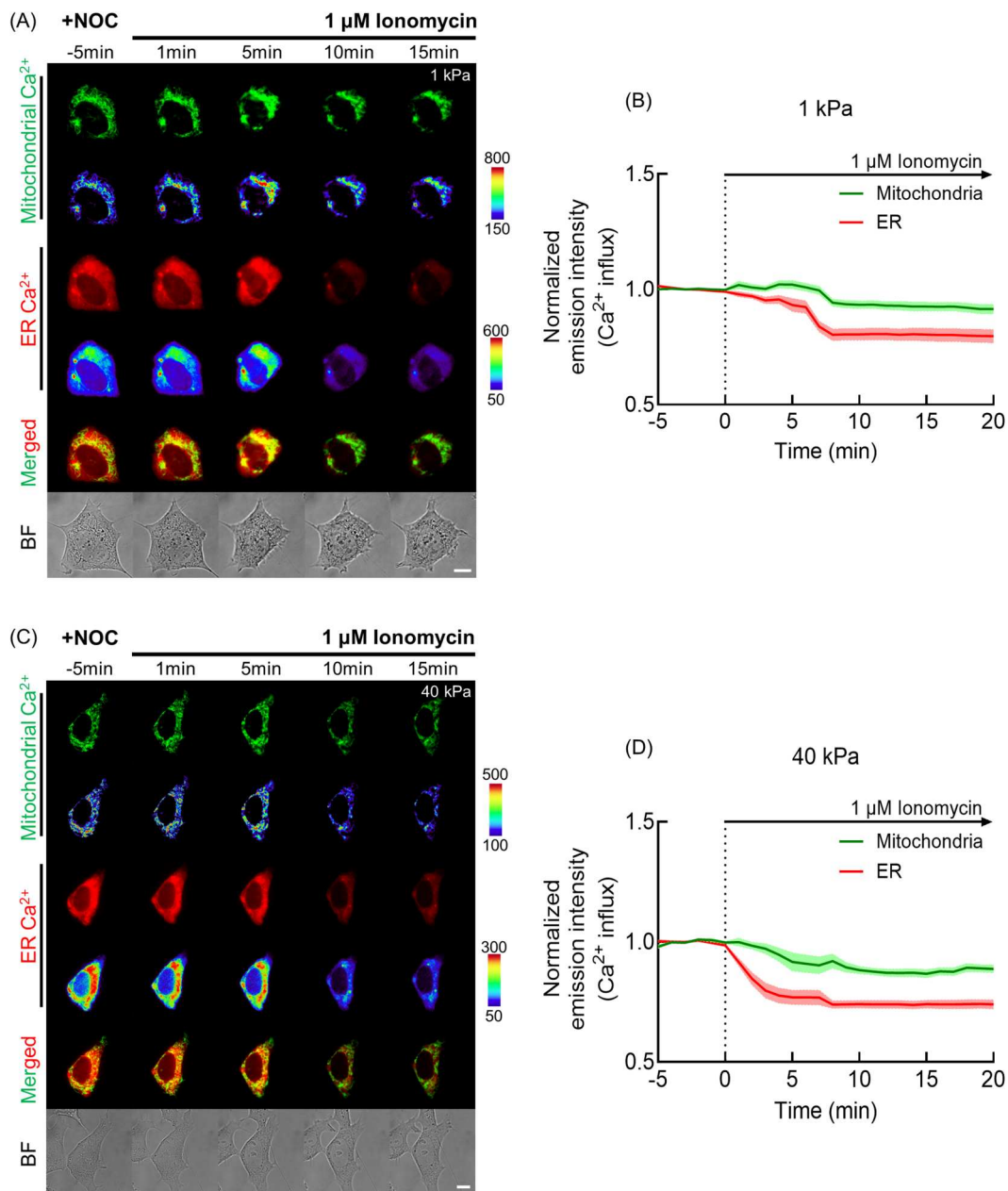


Figure 3. Influence of tubulin on mitochondrial calcium channel inhibition. (A, C) Live cell imaging illustrates the dynamics of the calcium indicators pCMV CEPIA2 mt (mitochondrial, green) and pCMV R-CEPIA1er (endoplasmic reticulum, red) in HeLa cells subjected to substrate stiffnesses of 1 and 40 kPa, respectively. Prior to ionomycin exposure, cells underwent a 30-min pre-treatment with 10 μM nocodazole, followed by a PBS wash. The application of 1 μM ionomycin was carried out subsequent to the commencement of live imaging, with only the cell media present during the initial 5 min. The color gradient bar highlights the calcium concentration, transitioning from high (red) to low (blue) levels (scale bar = 10 μm). (B) The time-dependent normalized emission intensities for mitochondrial (pCMV CEPIA2 mt) and ER (pCMV R-CEPIA1er) calcium sensors in HeLa cells on a 1 kPa substrate following 1 μM ionomycin treatment, representing average values across 11 cells ($n = 11$). (D) The normalized emission intensities over time for the same calcium sensors in cells on a 40 kPa substrate after 1 μM ionomycin application, representing average values across 10 cells ($n = 10$). Both (B) and (D) feature lines representing the mean normalized emission intensity, accompanied by error bars indicating the standard error of the mean (SEM), to highlight the impact of increased intracellular tubulin on mitochondrial calcium channel function under varying mechanical stiffness and ionomycin challenge.

CEPIA1er and pCMV CEPIA2 mt, to monitor Ca^{2+} levels in the mitochondria, ER, and HeLa cells to facilitate the observation of Ca^{2+} signaling. This method allows the selective visualization of intracellular organelles,

enabling real-time detection and observation of rapid changes in Ca^{2+} flow. Using live cells more accurately reflects the natural state of the cells, making our findings more generalizable.

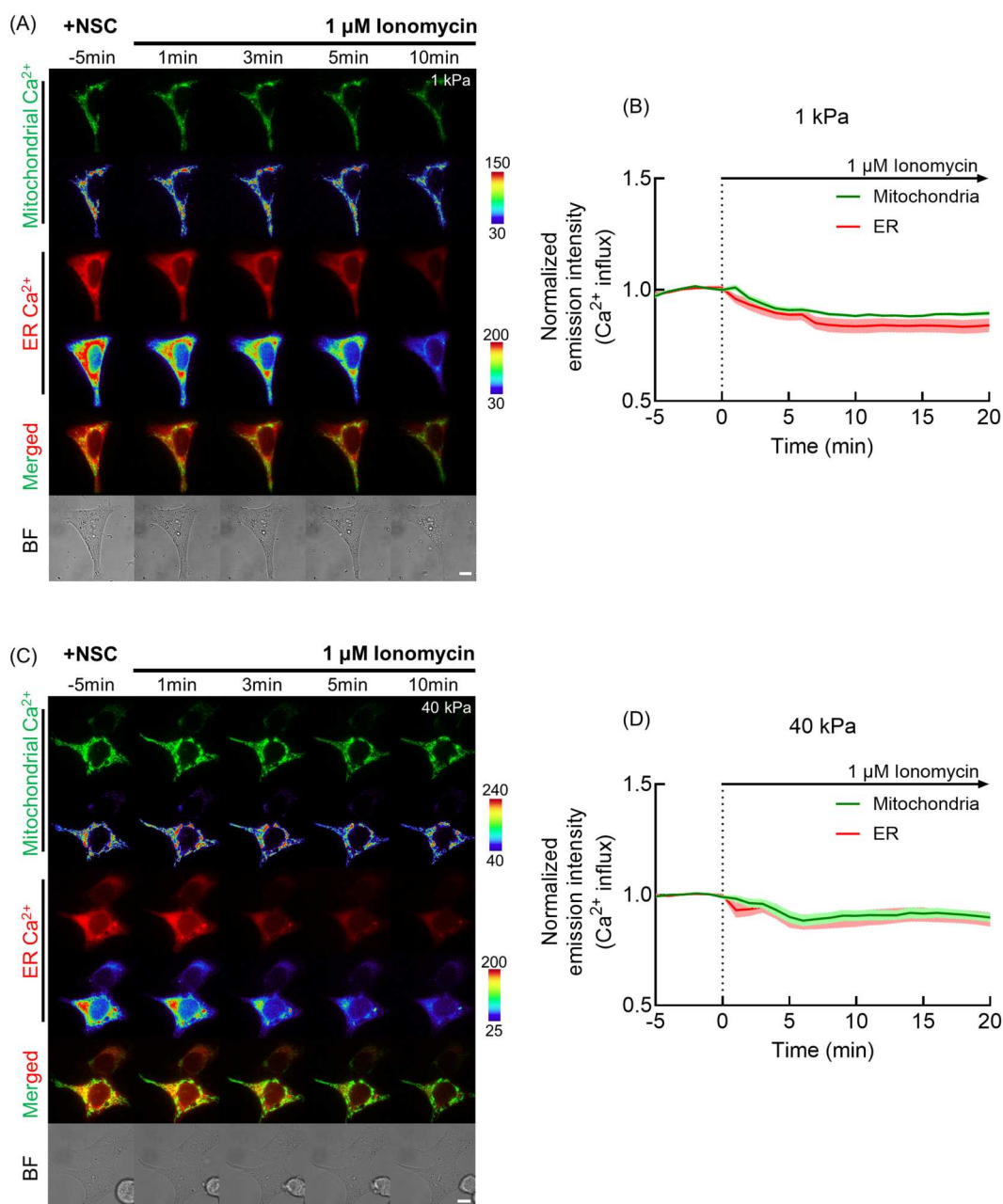


Figure 4. ECM stiffness modulates VDAC1 activity in mitochondrial calcium regulation. (A, C) Time-lapse images showing calcium flux within HeLa cells, visualized through calcium-specific biosensors: pCMV CEPIA2 mt for mitochondria (green) and pCMV R-CEPIA1er for the ER (red), across substrate stiffnesses of 1 and 40 kPa. Cells received pre-treatment with 10 μM NSC15364 for 1 h, followed by a PBS wash, and subsequent exposure to 1 μM ionomycin. Ionomycin application occurred after the initiation of live cell imaging, with only media and cells present in the confocal dish during the initial 5 min. The color scale bar reflects the concentration of Ca²⁺, with red indicating high and blue indicating low levels of Ca²⁺ (scale bar = 10 μm). (B) The normalized emission intensities from mitochondrial (pCMV CEPIA2 mt) and ER (pCMV R-CEPIA1er) calcium sensors in HeLa cells on a 1 kPa substrate post 1 μM ionomycin treatment, averaging data from nine cells (n = 9). (D) The normalized emission intensities over time for the same calcium indicators in HeLa cells on a 40 kPa substrate after 1 μM ionomycin treatment, with data averaged from 10 cells (n = 10). Both (B) and (D) feature lines representing the mean normalized emission intensities, with error bars denoting the standard error of the mean (SEM), highlighting the influence of ECM stiffness on VDAC1-mediated calcium influx into mitochondria under varying mechanical conditions and ionomycin treatment.

Using ionomycin to facilitate Ca²⁺ transfer from the ER to the mitochondria, we observed differential mitochondrial Ca²⁺ uptake between low (1 kPa) and high

(40 kPa) ECM stiffness conditions. Notably, increased uptake was evident at higher stiffness, despite similar levels of Ca²⁺ release from the ER under both conditions

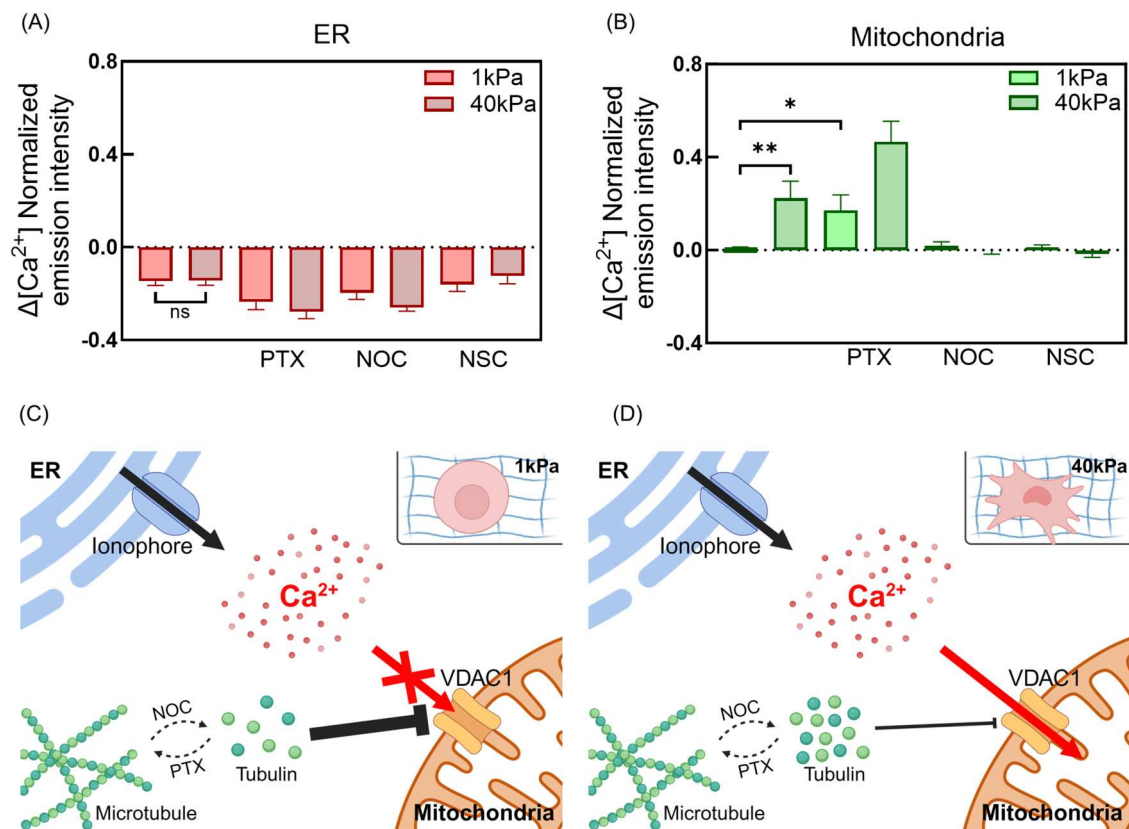


Figure 5. Differential impact of ECM stiffness and tubulin on ER and mitochondrial calcium dynamics. (A, B) The combined bar graph presents a comprehensive overview of the alterations in calcium levels within both the ER and mitochondria following treatment with 1 μ M ionomycin under varied experimental conditions. For ER calcium levels, the graph illustrates the average reduction in calcium by comparing the lowest normalized emission intensity post-ionomycin treatment to the baseline, indicating no significant deviation in calcium release from the ER across all conditions. Conversely, for mitochondrial calcium, the graph showcases the average increase by comparing the highest normalized emission intensity post-treatment to the baseline, highlighting significant variations in mitochondrial calcium uptake. To compare two independent groups, we used both unpaired t-tests and Mann-Whitney U tests, as appropriate, following normality and lognormality tests. Error bars across both datasets signify the standard error of the mean (SEM), with $**P < 0.01$ and $*P < 0.05$ marking statistical significance. Sequentially, the treatments include a control group (without any pretreatment), followed by cells pre-treated with paclitaxel, nocodazole, and NSC15364, across both 1 and 40 kPa substrate stiffness conditions. (C, D) A proposed model predicting how ECM stiffness modulates mitochondrial calcium channels. These models propose that VDAC1's activity is differentially influenced by tubulin depending on the substrate stiffness, leading to the observed variations in VDAC1 inhibition. This comprehensive analysis provides insight into the complex interplay between ECM stiffness, tubulin, and mitochondrial calcium regulation, demonstrating the regulatory mechanisms that govern cellular calcium dynamics in response to mechanical and biochemical cues.

(Figure 5). This led us to investigate whether the basal Ca^{2+} levels in the cell or Ca^{2+} channels in the mitochondria were affected by ECM stiffness. Since mitochondrial Ca^{2+} uptake is driven by membrane potential, if the levels of Ca^{2+} released from the ER are similar, a lower basal Ca^{2+} concentration inside the mitochondria should favor uptake (Duchen 2000). Our results showed that the basal level of mitochondrial Ca^{2+} was significantly higher at 40 kPa than at 1 kPa, suggesting that ECM hardness selectively modulates mitochondrial Ca^{2+} channels, thereby affecting Ca^{2+} uptake. Further investigation into the molecular underpinnings of this process led us to focus on the VDAC, which is critical for Ca^{2+} entry into the mitochondria and is subject to

regulation by its interaction with tubulin (Tomasello et al. 2009; Rostovtseva et al. 2012). Using paclitaxel, a microtubule stabilizer that reduces free intracellular tubulin, we found that lowering tubulin levels facilitated mitochondrial Ca^{2+} uptake at both stiffness levels, and significantly more so at 40 kPa (Figure 2; Nasrin et al. 2019). This suggests that tubulin acts as an inhibitor of VDAC, and its reduction by paclitaxel treatment activates these Ca^{2+} channels.

An intriguing aspect of our findings is the correlation between substrate stiffness and tubulin levels. Previous studies have highlighted that ECM stiffness influences tubulin levels (Kim et al. 2014; Fan et al. 2021). Despite the higher tubulin presence at 40 kPa compared to that

at 1 kPa, mitochondrial Ca^{2+} uptake was enhanced at higher stiffness levels, indicating that ECM stiffness modulates the regulatory impact of tubulin on mitochondrial Ca^{2+} uptake. Lower stiffness results in diminished tubulin levels but exerts a disproportionately significant influence on the regulatory role of tubulin. To validate these findings, we explored the effects of increased intracellular tubulin levels on mitochondrial Ca^{2+} channels using nocodazole, a microtubule-depolymerizing agent that increases free tubulin levels (Iwamoto et al. 2017). Enhancing tubulin levels through nocodazole treatment, followed by ionomycin application, led to an increase in ER Ca^{2+} release, but failed to elevate mitochondrial Ca^{2+} uptake across both stiffness levels (Figure 5). These findings support the hypothesis that increased intracellular tubulin levels inhibit VDAC.

Focusing on VDAC1 isoforms, which are critical for mitochondrial Ca^{2+} entry, we used NSC15364, a selective inhibitor of VDAC1 that prevents its oligomerization. The inhibition of VDAC1 markedly reduced mitochondrial Ca^{2+} uptake following ionomycin-induced ER Ca^{2+} release, irrespective of ECM stiffness (Figure 5). This indicates that VDAC1 is the primary conduit for mitochondrial Ca^{2+} entry and is influenced by tubulin levels. Our findings highlighted the regulatory axis involved in ECM stiffness, tubulin modulation, and VDAC1 activity. Higher ECM rigidity facilitates greater mitochondrial Ca^{2+} uptake than lower stiffness owing to the differential influence of tubulin on VDAC1. Increased tubulin levels at lower ECM stiffness inhibited the channel more effectively, thereby attenuating mitochondrial Ca^{2+} uptake.

In conclusion, our study underscores the significance of the mechanical microenvironment, represented by ECM stiffness in concert with the cytoskeletal element tubulin, in the modulation of intracellular Ca^{2+} dynamics via VDAC1. These interactions provide novel insights into the regulatory mechanisms governing cellular Ca^{2+} homeostasis. Understanding the dependence of intracellular Ca^{2+} mechanisms on ECM stiffness enriches our understanding of cellular physiology and opens new avenues for the development of targeted therapeutic strategies. Specifically, manipulating the TME components and Ca^{2+} signaling pathways holds the potential for advancing therapeutic interventions. While our study provides significant insights, potential weaknesses include the use of only one cell type (HeLa cells) and the focus on non-excitabile cells, which may limit the generalizability of our findings. Literature suggests that different cell types, including excitable cells like neurons and muscle cells, may exhibit different Ca^{2+} signaling mechanisms. Future experiments should include a variety of cell types to verify if the observed mechanisms are universal.

Author contributions

Minji Kim and Tae-Jin Kim conceptualized the project, designed the experiments, and wrote the manuscript. Minji Kim performed the experiments and analyzed the data. Kiseok Han, Gyuho Choi, Sanghyun Ahn, and Jung-Soo Suh analyzed the data. All authors contributed to the discussion. All the authors have read and approved the final version of this manuscript.

Disclosure statement

No potential conflict of interest was reported by the author(s).

Funding

This study was supported by grants from the National Research Foundation of Korea (NRF) [grant nos. 2022R1A4A5031503, RS-2023-00279771 and RS-2024-00400827].

ORCID

Tae-Jin Kim  <http://orcid.org/0000-0001-7678-0478>

References

- Ashrafi G, de Juan-Sanz J, Farrell RJ, Ryan TA. 2020. Molecular tuning of the axonal mitochondrial Ca^{2+} uniporter ensures metabolic flexibility of neurotransmission. *Neuron*. 105(4):678–687.e5. doi:10.1016/j.neuron.2019.11.020.
- Ben-Hail D, Begas-Shvartz R, Shalev M, Shteinifer-Kuzmine A, Gruzman A, Reina S, De Pinto V, Shoshan-Barmatz V. 2016. Novel compounds targeting the mitochondrial protein VDAC1 inhibit apoptosis and protect against mitochondrial dysfunction. *J Biol Chem*. 291(48):24986–25003. doi:10.1074/jbc.M116.744284.
- Deng B, Zhao Z, Kong W, Han C, Shen X, Zhou C. 2022. Bilirubin ameliorates murine atherosclerosis through inhibiting cholesterol synthesis and reshaping the immune system. *J Transl Med*. 20(1):1–15. doi:10.1186/s12967-021-03207-4.
- De Stefani D, Bononi A, Romagnoli A, Messina A, De Pinto V, Pinton P, Rizzuto R. 2012. VDAC1 selectively transfers apoptotic Ca^{2+} signals to mitochondria. *Cell Death Differ*. 19(2):267–273. doi:10.1038/cdd.2011.92.
- Duchen MR. 2000. Mitochondria and calcium: from cell signaling to cell death. *J Physiol*. 529(1):57–68. doi:10.1111/j.1469-7793.2000.00057.x.
- Fan Y, Sun Q, Li X, Feng J, Ao Z, Li X, Wang J. 2021. Substrate stiffness modulates the growth, phenotype, and chemoresistance of ovarian cancer cells. *Front Cell Dev Biol*. 9 (August):1–13. doi:10.3389/fcell.2021.718834.
- Franklin JM, Ghosh RP, Shi Q, Reddick MP, Liphardt JT. 2020. Concerted localization-resets precede YAP-dependent transcription. *Nat Commun*. 11(1):1–18. doi:10.1038/s41467-020-18368-x.
- Giorgi C, Bonora M, Missiroli S, Poletti F, Ramirez FG, Morciano G, Morganti C, Pandolfi PP, Mammano F, Pinton P. 2015. Intravital imaging reveals p53-dependent cancer cell death

- induced by phototherapy via calcium signaling. *Oncotarget*. 6(3):1435–1445. doi:10.18632/oncotarget.2935.
- Giorgi C, Marchi S, Pinton P. 2018. The machineries, regulation and cellular functions of mitochondrial calcium. *Nat Rev Mol Cell Biol*. 19(11):713–730. doi:10.1038/s41580-018-0052-8.
- Hotka M, Cagalinec M, Hilber K, Hool L, Boehm S, Kubista H. 2020. L-type Ca²⁺ channel-mediated Ca²⁺ influx adjusts neuronal mitochondrial function to physiological and pathophysiological conditions. *Sci Signal*. 13(618):1–15. doi:10.1126/scisignal.aaw6923.
- Ichas F, Jouaville LS, Mazat JP. 1997. Mitochondria are excitable organelles capable of generating and conveying electrical and calcium signals. *Cell*. 89(7):1145–1153. doi:10.1016/S0092-8674(00)80301-3.
- Iwamoto M, Cai D, Sugiyama M, Suzuki R, Aizaki H, Ryo A, Ohtani N, Tanaka Y, Mizokami M, Wakita T, et al. 2017. Functional association of cellular microtubules with viral capsid assembly supports efficient hepatitis B virus replication. *Sci Rep*. 7(1):1–10. doi:10.1038/s41598-016-0028-x.
- Kerkhofs M, Bittremieux M, Morciano G, Giorgi C, Pinton P, Parys JB, Bultynck G. 2018. Emerging molecular mechanisms in chemotherapy: Ca²⁺ signaling at the mitochondria-associated endoplasmic reticulum membranes. *Cell Death Dis*. 9(3). doi:10.1038/s41419-017-0179-0.
- Kim J, Seo S, Park J H Y, Lee K W, Kim J, Kim J C. 2023. Ca²⁺-permeable TRPV1 receptor mediates neuroprotective effects in a mouse model of Alzheimer's disease via BDNF/CREB signaling pathway. *Molecules and cells*. 46(5):319–328.
- Kim J B, Bae J E, Park N Y, Jo D S, Kim Y H, Jeong K, Cho ... 2023. Inhibition of ubiquitin specific peptidase 14 (USP14) promotes ER-phagy by inducing ER stress in human hepatoma HepG2 cells. *Animal Cells and Systems*. 27(1):394–402.
- Kim T J, Seong J, Ouyang M, Sun J, Lu S, Hong J P, Wang ... 2009. Substrate rigidity regulates Ca²⁺ oscillation via RhoA pathway in stem cells. *Journal of cellular physiology*. 218(2):285–293.
- Kim TJ, Sun J, Lu S, Zhang J, Wang Y. 2014. The regulation of β -adrenergic receptor-mediated PKA activation by substrate stiffness via microtubule dynamics in human MSCs. *Biomaterials*. 35(29):8348–8356. doi:10.1016/j.biomaterials.2014.06.018.
- Kwon J, Kim J, Kim K. 2023. Crosstalk between endoplasmic reticulum stress response and autophagy in human diseases. *Animal Cells Syst (Seoul)*. 27(1):29–37. doi:10.1080/19768354.2023.2181217.
- Maldonado EN, Patnaik J, Mullins MR, Lemasters JJ. 2010. Free tubulin modulates mitochondrial membrane potential in cancer cells. *Cancer Res*. 70(24):10192–10201. doi:10.1158/0008-5472.CAN-10-2429.
- Missiroli S, Patergnani S, Carocchia N, Pedriali G, Perrone M, Previati M, Wieckowski MR, Giorgi C. 2018. Mitochondria-associated membranes (MAMs) and inflammation. *Cell Death Dis*. 9(3). doi:10.1038/s41419-017-0027-2.
- Monteith GR, Prevarskaya N, Roberts-Thomson SJ. 2017. The calcium-cancer signalling nexus. *Nat Rev Cancer*. 17(6):373–380. doi:10.1038/nrc.2017.18.
- Nasrin SR, Rashedul Kabir AM, Konagaya A, Ishihara T, Sada K, Kakugo A. 2019. Stabilization of microtubules by cevipabulin. *Biochem Biophys Res Commun*. 516(3):760–764. doi:10.1016/j.bbrc.2019.06.095.
- Oh BC. 2023. Phosphoinositides and intracellular calcium signaling: novel insights into phosphoinositides and calcium coupling as negative regulators of cellular signaling. *Exp Mol Med*. 55(8):1702–1712. doi:10.1038/s12276-023-01067-0.
- Ojeda-Lopez MA, Needleman DJ, Song C, Ginsburg A, Kohl PA, Li Y, Miller HP, Wilson L, Raviv U, Choi MC, Safinya CR. 2014. Transformation of taxol-stabilized microtubules into inverted tubulin tubules triggered by a tubulin conformation switch. *Nat Mater*. 13(2):195–203. doi:10.1038/nmat3858.
- Park JH, Jo SB, Lee JH, Lee HH, Knowles JC, Kim HW. 2023. Materials and extracellular matrix rigidity highlighted in tissue damages and diseases: implication for biomaterials design and therapeutic targets. *Bioactive Materials*. 20 (June 2022):381–403. doi:10.1016/j.bioactmat.2022.06.003.
- Patergnani S, Suski JM, Agnoletto C, Bononi A, Bonora M, De Marchi E, Giorgi C, Marchi S, Missiroli S, Poletti F, et al. 2011. Calcium signaling around mitochondria associated membranes (MAMs). *Cell Commun Signal*. 9:1–10. doi:10.1186/1478-811X-9-19.
- Rostovtseva TK, Gurnev PA, Chen MY, Bezrukov SM. 2012. Membrane lipid composition regulates tubulin interaction with mitochondrial voltage-dependent anion channel. *J Biol Chem*. 287(35):29589–29598. doi:10.1074/jbc.M112.378778.
- Seegren PV, Harper LR, Downs TK, Zhao XY, Viswanathan SB, Stremaska ME, Olson RJ, Kennedy J, Ewald SE, Kumar P, Desai BN. 2023. Reduced mitochondrial calcium uptake in macrophages is a major driver of inflammaging. *Nature Aging*. 3(7):796–812. doi:10.1038/s43587-023-00436-8.
- Seong J, Ouyang M, Kim T, Sun J, Wen PC, Lu S, Zhuo Y, Llewellyn NM, Schlaepfer DD, Guan JL, et al. 2011. Detection of focal adhesion kinase activation at membrane microdomains by fluorescence resonance energy transfer. *Nat Commun*. 2(1). doi:10.1038/ncomms1414.
- Spencer W, Kwon H, Crépieux P, Leclerc N, Lin R, Hiscott J. 1999. Taxol selectively blocks microtubule dependent NF- κ B activation by phorbol ester via inhibition of I κ B α phosphorylation and degradation. *Oncogene*. 18(2):495–505. doi:10.1038/sj.onc.1202335.
- Suzuki J, Kanemaru K, Ishii K, Ohkura M, Okubo Y, Iino M. 2014. Imaging intraorganellar Ca²⁺ at subcellular resolution using CEPIA. *Nat Commun*. 5(May):1–13. doi:10.1038/ncomms5153.
- Tomasello F, Messina A, Lartigue L, Schembri L, Medina C, Reina S, Thoraval D, Crouzet M, Ichas F, De Pinto V, De Giorgi F. 2009. Outer membrane VDAC1 controls permeability transition of the inner mitochondrial membrane in cellulose during stress-induced apoptosis. *Cell Res*. 19(12):1363–1376. doi:10.1038/cr.2009.98.
- Wu NN, Wang L, Wang L, Xu X, Lopaschuk GD, Zhang Y, Ren J. 2023. Site-specific ubiquitination of VDAC1 restricts its oligomerization and mitochondrial DNA release in liver fibrosis. *Exp Mol Med*. 55(1):269–280. doi:10.1038/s12276-022-00923-9.
- Zamaraeva MV, Sabirov RZ, Manabe K, Okada Y. 2007. Ca²⁺-dependent glycolysis activation mediates apoptotic ATP elevation in HeLa cells. *Biochem Biophys Res Commun*. 363(3):687–693. doi:10.1016/j.bbrc.2007.09.019.
- Zhang S, Zeng L, Su B, Yang G, Wang J, Ming S, Chu B. 2023. The glycoprotein 5 of porcine reproductive and respiratory syndrome virus stimulates mitochondrial ROS to facilitate viral replication. *Vet Microbiol*. 14(6):1–21.